

# **STRUCTURAL INTEGRITY INVESTIGATION OF SAC305 LEAD FREE SOLDER**

by

**EESVARAN A/L GANIASHAN**

**(Matrix No.: 144350)**

**Supervisor**

**Assoc. Prof. Dr Abdullah Aziz Saad**

**2022**

This dissertation is submitted to  
Universiti Sains Malaysia  
As partial fulfillment of the requirement to graduate with honors degree in  
**BACHELOR OF ENGINEERING (MECHANICAL ENGINEERING)**



## DECLARATION

This work has not previously have been accepted in substance for any degree and is not being concurrently submitted in candidature for any degree. Statement 1: This journal is the result of my own investigation, except where otherwise stated. Other sources are acknowledged by giving explicit references. Bibliography/ references are appended. Statement 2: I hereby give consent for my journal, if accepted, to be available for photocopying and for interlibrary loan, and for the title and summary to be made available outside organizations.

.....*Eesvaran*.....

(EESVARAN A/L GANIASHAN)

Date: 24/7/2022

## **ACKNOWLEDGEMENT**

First, I'd like to say thanks to my supervisor, Assoc. Prof. Dr. Abdullah Aziz Saad, for his outstanding contributions, outstanding support, dedication, and tolerance throughout this project. His advice is deeply appreciated, and I am convinced that one could not have progressed this far without such close supervision. My supervisor's advice and encouragement have always kept me motivated and helped me overcome obstacles.

Next, I'd like to thank the School of Mechanical Engineering at Universiti Sains Malaysia for providing the necessary equipment to complete my Final Year Project (FYP). I am grateful for the opportunity to pursue this four-year degree in Mechanical Engineering, and I am confident that the knowledge and technical skills I have gained will be extremely useful in my future career as an engineer. In addition, I'd like to thank the School of Materials and Mineral Resources Engineering at Universiti Sains Malaysia for accommodating me and allowing me to use their facilities and equipment during my studies. Special thanks go to all academic and technical staff for their hard work and valuable collaboration.

Furthermore, I would like to thank Assoc. Prof. Dr. Ahmad Azmin Mohamad for his willingness to share his expertise and knowledge with me, as well as his willingness to assist me whenever necessary. Despite their extremely busy schedules, they were willing to take time out to listen to, lead, and guide me through the completion of my project. Finally, I'd like to express my gratitude to my supportive family and friends for their unending encouragement and support throughout my project. I could not have completed this project without the advice, opinions, and constructive criticism I received during this time.

## TABLE OF CONTENTS

<b>AKNOWLEDGEMENT</b> .....	III
<b>LIST OF TABLES</b> .....	VI
<b>LIST OF FIGURES</b> .....	VII
<b>LIST OF ABBREVIATIONS</b> .....	IX
<b>ABSTRAK</b> .....	X
<b>ABSTRACT</b> .....	XI
<b>CHAPTER 1</b> .....	1
<b>INTRODUCTION</b> .....	1
<b>1.1 Overview</b> .....	1
<b>1.2 Research Background</b> .....	2
<b>1.3 Problem Statement</b> .....	3
<b>1.4 Objective</b> .....	4
<b>1.5 Scope of Work</b> .....	4
<b>CHAPTER 2</b> .....	5
<b>LITERATURE REVIEW</b> .....	5
<b>2.1 Introduction</b> .....	5
<b>2.2 Lead Free Solder Alloys</b> .....	5
<b>2.3 Types of SAC Solders (SAC305, SAC387, SAC405, SAC0307)</b> .....	10
<b>2.4 Soldering Technique</b> .....	11
<b>2.3.1 Reflow Soldering</b> .....	12
<b>2.3.2 Wave Soldering</b> .....	15
<b>2.4 Intermetallic compound (IMC) layer</b> .....	16
<b>2.5 Hardness Test</b> .....	18
<b>2.5.1 Vickers Hardness Test</b> .....	19
<b>2.5.2 Microhardness</b> .....	21
<b>2.5.3 Nanohardness</b> .....	24
<b>CHAPTER 3</b> .....	28
<b>METHODOLOGY</b> .....	28
<b>3.1 Introduction</b> .....	28

<b>3.2 List of materials and equipment</b> .....	28
<b>3.3 Preparation of SAC305 composite solder</b> .....	29
<b>3.4 Solder Reflow</b> .....	30
<b>3.5 Sample preparation for characterization by SEM, XRD and Nano Indenter.</b>	31
<b>3.6 Analysis Materials Characterization</b> .....	34
<b>3.6.1 Phase Determination</b> .....	34
<b>3.6.2 Microstructural and Compositional Analysis</b> .....	35
<b>3.6.3 Hardness test</b> .....	35
<b>3.7 Flow Chart</b> .....	36
<b>CHAPTER 4</b> .....	37
<b>RESULT AND DISCUSSION</b> .....	37
<b>4.1 Introduction</b> .....	37
<b>4.2 Characterization of Sn-Ag-Cu solder on Cu Substrate and Intermetallic Compounds after Solder Reflow.</b> .....	37
<b>4.2.1 Surface Appearance</b> .....	37
<b>4.2.2 Morphology Evolution</b> .....	38
<b>4.2.3 Phase Determination</b> .....	42
<b>4.3 Hardness Test</b> .....	44
<b>4.3.1 Vickers Hardness</b> .....	44
<b>4.3.2 Nano Indentation</b> .....	46
<b>CHAPTER 5</b> .....	51
<b>CONCLUSION AND FUTURE RECOMMENDATIONS</b> .....	51
<b>5.1 Conclusion</b> .....	51
<b>5.2 Recommendation for future research.</b> .....	52
<b>REFERENCE</b> .....	53

## LIST OF TABLES

Table 2.1 Hardness and tensile properties of lead-free solders (Smith & Madeni, 2002) ...	7
Table 2.2 The effect of alloy elements on the corrosion of Sn-based lead-free solder alloys (Li et al., 2020).....	8
Table 2.3 Types of SAC Alloys.....	10
Table 3.1: Surface diameter for every cross section of the solder samples .....	34
Table 4.1: Data recorded for the Vickers Hardness of all the reflowed SAC305/Cu solder sample with the same parameters (220°C and 60s) at five different point. ....	44
Table 4.2: Cross-sectional measurements of average depth displacements and average hardness values. ....	47

## LIST OF FIGURES

Figure 2. 1: Diagram of Solder on Cu substrate (Comparing Mechanical and Soldering Properties of Alternative Lead-Free Alloys   AIM Solder, n.d.).....	12
Figure 2. 2: A typical reflow profile (Huang & Lin, 2013) .....	14
Figure 2. 3 : Temperature and time graph shows the wave soldering solder pot and the temperatures of the topside (Barbini et al., 2007).....	15
Figure 2. 4: SEM image of Intermetallic Compound (Chan et al., 1997).....	17
Figure 2. 5: Vickers Hardness Test indenter geometry. Image is © 2017 EngineeringClicks .....	19
Figure 2. 6: Vickers Hardness Test indentation examples. Image is © 2017 EngineeringClicks.....	20
Figure 2. 7: Bar graph showing the impact of TiO <sub>2</sub> nanoparticles on its microhardness of the Sn <sub>3.5</sub> AgXCu solders (Chang et al., 2011).....	22
Figure 2. 8: The graph showing the effect on the addition of TiO <sub>2</sub> nanoparticle on the microhardness of the Sn–3.0Ag–0.5Cu–xTiO <sub>2</sub> composite solders (Tang et al., 2014). ...	23
Figure 2. 9: Results of nanohardness: a) Nano hardness value of Sn-3.0Ag-0.5Cu interface (Lutfi et al., 2015), b) The hardness and the modulus of SAC, SAC-Ni. and SAC-Bi solders measured using nanoindentation (Lin et al., 2018), Hardness profiles of the solder alloys (Shareeda et al., 2019), Nano hardness of the Sn-rich phase and the Bi-rich phase in the bulk solders (Yang et al., 2020). .....	25
Figure 3. 2: (a) Microwave Oven (b) SAC305/Cu sample inside microwave oven .....	30
Figure 3. 3: Flow chart of solder reflowing .....	30
Figure 3. 4: (a) Reflowed solder sample, (b) Top view of reflowed solder sample on copper substrate .....	31
Figure 3. 5: Schematic for different cross sections of the solder.....	32
Figure 3. 6: Examples of different horizontal cross section of the solder .....	33
Figure 3. 7: Schematic Diagram for measurement point for nano-indenter test.....	35
Figure 3. 8: Flow Chart of the Experiment .....	36
Figure 4. 1: (a) as-deposited SAC305, and (b) reflowed SAC305/C at 220 °C for 60 s. ...	38

Figure 4. 2: Examples of different horizontal cross section of the solder (a) CS-1, (b) CS-2 , (c) CS-3, (d) CS-4.....	39
Figure 4.3: Morphology of the pure SAC305 solder alloy at (a) .CS-1 region, (b) .CS-2 region, (c) .CS-3 region, (d) .CS-4 region .....	40
Figure 4. 4: EDX of the reflowed SAC305 solder alloy at (a) CS-1. region, (b) CS-2. region, (c) CS-3. region, (d) CS-4. Region. ....	41
Figure 4.5 XRD pattern of reflowed SAC305 solder on Cu substrate for 4 cross-sections .....	42
Figure 4.6: Average Vickers Hardness of reflowed SAC305/Cu solder .....	45
Figure 4.7: Schematic diagram of intermetallic compound phases at different horizontal cross section of the solder (a) .CS-1 region, (b) .CS-2 region, (c) .CS-3 region, (d) .CS-4 region .....	46
Figure 4.8: Average Hardness of reflowed SAC305/Cu solder.....	47
Figure 4. 9: Indentation curves of the SAC305 solder alloy at (a) .CS-1, (b) .CS-2, (c) CS-3 and (d) .CS-4 regions .....	49
Figure 4.10: the IMC phase improve the hardness at the CS-4 can be seen under the SEM results .....	50

## LIST OF ABBREVIATIONS

PCB	Printed Circuit Board
SAC305	96.5Sn-3.0Ag-0.5Cu
NaCl	Sodium Chloride
IMC	Intermetallic Compound
BGA	Ball Grid Array
SEM	Scanning Electron Microscopy
XRD	X-Ray Diffraction
PWB	Printed Wiring Board
SMT	Surface Mount Technology
IR	Infrared
EDS	Energy Dispersive Spectroscopy
EDX	Energy Dispersive X-Ray
FESEM	Field Emission Scanning Electron Microscopy
ICDD	International Centre of Diffraction Data

# SIASATAN INTEGRITI STRUKTUR PATERI BEBAS PLUMBUM SAC305

## ABSTRAK

Penambahbaikan dalam kekuatan pateri serta-merta menjadi salah satu kebimbangan paling penting dalam industri elektronik, terutamanya dalam aplikasi Papan Litar Bercetak (PCB). Kerana reka bentuk dan pemasangan komponen elektronik pada substrat atau PCB, pateri dalam sambungan elektronik mungkin retak dan berubah bentuk kepada faktor tertentu. Ini menyebabkan kegagalan peranti dan kos yang besar, dan kesan sebenar retak yang menyebabkan kerugian dalam sektor perindustrian tidak dimaklumkan secara meluas. Akibatnya, kekuatan mekanikal pateri kini menjadi salah satu isu yang paling rumit, dan ia telah mendapat perhatian yang meningkat dalam beberapa tahun kebelakangan ini hasil daripada peningkatan jaminan produk, teknologi canggih dan perubahan fasa yang disebabkan oleh undang-undang terkini yang mempengaruhi sektor elektronik. Di samping itu, ciri pateri SAC305 yang halus dan belum dipelajari pada tembaga adalah terhad. Oleh itu, projek ini dijalankan untuk mengkaji sifat mekanikal pateri SAC305. Pateri filem nipis SAC305/Cu yang dialirkan semula dengan suhu 220 °C pada 60 saat telah disiasat. Struktur mikro, fasa struktur, dan kekerasan sebatian antara logam yang terbentuk telah disiasat. IMC antara muka yang terbentuk antara SAC305 dan substrat Cu selepas pengaliran semula pateri ialah Cu<sub>6</sub>Sn<sub>5</sub> dan Ag<sub>3</sub>Sn. IMC boleh dilihat dalam SEM dan dikesan dalam XRD. Kesan IMC dari segi kekerasan telah disiasat menggunakan ujian kekerasan Vickers dan nanoindentation. Tatasusunan lekukan tertentu telah dilakukan pada empat keratan rentas mendatar yang berbeza pada pateri dengan ketinggian dan diameter yang berbeza. Nilai kekerasan meningkat secara beransur-ansur dari keratan rentas atas ke arah bersebelahan dengan antara muka pateri/substrat.

# **STRUCTURAL INTEGRITY INVESTIGATION OF SAC305 LEAD FREE SOLDER**

## **ABSTRACT**

Improvement in solder strength is instantly becoming one of the most important concerns in the electronics industry, particularly in Printed Circuit Board (PCB) applications. Because of the design and mounting of electronic components on a substrate or PCB, solder in electronic connections may crack and deform to certain factors. These causes device failures and massive costs, and the true impact of crack caused losses in the industrial sector is not widely communicated. As a result, mechanical strength of solder is now one of the most complicated issues, and it has received increased attention in recent years as a result of increased product warranties, advanced technologies, and phase changes brought about by recent laws affecting the electronics sector. In addition, a delicate and unstudied characteristic of SAC305 solder on copper was limited. Therefore, this project was conducted to study the mechanical properties of SAC305 solder. The reflowed SAC305/Cu solder with the temperature of 220°C at 60 seconds was investigated. The microstructure, structural phase, and hardness of the formed intermetallic compounds were investigated. The interfacial IMC formed between SAC305 and the Cu substrate after solder reflow is  $\text{Cu}_6\text{Sn}_5$  and  $\text{Ag}_3\text{Sn}$ . The IMCs were visible in SEM and detected in XRD. The effect of IMCs in the terms of hardness was investigated using Vickers hardness test and nanoindentation. A specific indentation array was performed on four different horizontal cross sections of the solder with different heights and diameters. The hardness values increased gradually from the top cross sections towards adjacent to the solder/substrate interface.

# CHAPTER 1

## INTRODUCTION

### 1.1 Overview

Electrical components are mostly joint with solder alloy paste to give electronic connection in industries. The demand for dependability has grown significantly along with the significant expansion in the usage of electronics. Serious corrosion issues have been caused by the need for downsizing, the diversity of materials employed, the impact of process wastes, and the unpredictable user environment. One industry where the user environment varies greatly is consumer electronics. Electronic devices are currently getting smaller overall at a quicker rate. In electronic industries, Sn-Pb solders are mostly used. These is because Sn-Pb is good resistance for corrosion, lower cost and mechanical properties. However, Pb is a heavy toxin metal that is dangerous to health and the environment. So that, many research start to investigate on lead free solders to replace the Sn-Pb solders. When the device with lead free solder is in use, the industries have started to face problems in terms of wettability, mechanical performance and also corrosion.

With the development of microelectronic packaging and the increasingly specific service environment of solder joints, the properties of Pb free solders have been studied and very strictly required. In this era, nanoparticles have been used to improve the microstructure and properties of lead-free solders due to their small size effect and high surface energy. As a result, nanoparticle enhanced composite solders have recently gained very good attentions and results. This article reviewed recent research on SnAgCu, SnBi, and SnZn composite solder alloys and discussed how nanoparticles affect their microstructure, mechanical properties, wettability, and reliability.

## 1.2 Research Background

As technology has become an integral part of our daily lives, printed circuit boards (PCB) play an increasingly important role. Because they have been used in all electrical and electronic devices and also circuit boards. Because they are at the heart of the majority of electrical devices today, they can come in a variety of configurations that allow them to serve a variety of purposes and perform multiple functions. Most home appliances and entertainment systems, whether they are a mobile phone, a computer, a microwave, or even a coffee maker, contain a circuit board. As technology advances and evolves, so will the demand for PCBs. However, the disadvantages of these advanced technologies include the susceptibility of electronic devices to humidity and contaminants, as well as corrosion failure (Yi et al., 2015)

The current lead-free solder development has resulted in the development of new variations in solder alloy formulations. Several characterizations and tests are used to evaluate the developed solder alloy, including phase analysis, corrosion resistance, morphological behavior and mechanical properties. Mechanical testing for tensile, shear, and hardness value is one of the most important indicators used to determine the performance of Pb free solders, and as such, it has obtained the interest of academics and researchers.(Yahaya & Mohamad, 2017)

The preferred methods for mechanically evaluating a solder alloy include Vickers hardness, Brinell hardness, and nanoindentation test.(Yahaya et al., 2016) The Vickers and Brinell hardness allow for the direct measurement of hardness values. This type of access is beneficial and acts as a first level of examination before further characterization. Methods like nanoindentation enable dynamic load control measurements while also providing additional analysis and information.

Mechanical properties are very important, and the development of nano-composite solders (which contain a little quantity of metallic or ceramic nanoparticles into the SAC solder) provides huge potential for improving mechanical performance. The addition of TiO<sub>2</sub> nanoparticles improves the SAC's mechanical properties significantly. The refined - Sn, Cu<sub>6</sub>Sn<sub>5</sub>, and Ag<sub>3</sub>Sn IMC phases were linked to such improvements in mechanical

properties. This is possible because the increased grain boundaries due to smaller grains size provides more dislocation movements, improving the solder alloys' resistance to deform.(Shareeda et al., 2019).

### **1.3 Problem Statement**

Nowadays, ternary Pb free solder alloys have been mostly used in most of electronic assemblies. Corrosion damage to the PCB surface is the root cause of decreased reliability and product lifetime. Corrosion occurs on soldered connections when they are exposed to atmospheric moisture. Besides air, the solder will meet moisture and corrosive agents such as sulfur and chlorine. Corrosion products are made up of a wide range of oxide compounds with varying physical properties. These oxide mixtures can cause a variety of electronic failures, including interruptions and shorts. Corrosion in electronic equipment can also result in faulty contact lines and connection loss.

Then, the large volume fraction of  $Ag_3Sn$  intermetallic compound (IMC) and quick reaction rate with the metallization layer however remains as the fundamental disadvantage of the Sn-3.0Ag-0.5Cu. The intermetallic (IMC) layer grows more quickly in SAC than it did in alloys containing lead pb, which lowers the mechanical performance of the joints as a result it causes brittle fractures, shortening cycle and thermal fatigue life, and being more susceptible to plastic deformation.

A solder alloy must have higher hardness properties. In this project, the hardness of SAC solder alloy will be evaluated by nanoindentation. Indentation test will be performed with four different horizontal cross sections of the composite solder with different diameters and heights. Hence the higher level of hardness properties will be obtained by the Sn-Ag-Cu solder alloy.

## **1.4 Objective**

1. To fabricate the SAC305 solder on copper substrate by using conventional reflow soldering method.
2. To characterize reflowed SAC305/Cu solder by using Scanning Electron Microscopy (SEM), X-Ray Diffraction (XRD), Vickers Hardness and Nano Indenter.

## **1.5 Scope of Work**

In this experiment, lead-free SAC 305 solder paste was used to form a solder joint between SAC 305 solder and the copper substrate. This project involves on preparing samples of SAC305 solder on Cu substrate, and the second section involves characterising the SAC305 solder on Copper substrate following the reflow soldering process. This step ensures that the IMC develops at the interface. The structural and microstructural characteristics of samples were identified and evaluated for each cross-section. The research focuses on the structural and microstructural properties SAC 305 solder. Other than that, this research will look into the corrosion impact on the solder joint between the SAC305 solder and the copper substrate. In this study, characterization tools such as a scanning electron microscope (SEM) and X-Ray Diffraction (XRD) were also used to determine the structure of the joining of the solder formation.

## **CHAPTER 2**

### **LITERATURE REVIEW**

#### **2.1 Introduction**

This topic discusses the significance of SAC solder and the intermetallic compound IMC layer in the electronics industry, as there have been few studies on the thin film characteristics of this alloy. As a result, the interfacial reaction of this alloy is examined using the reflow soldering process on a Cu substrate. An addition there also has a review on wave soldering. This literature review also presented in order to develop a theoretical framework for the effect of corrosion on Printed Circuit Board, electronic devices and also the range of hardness and strength of solder alloys. Journals, papers, technical reports, and other publications summarized in this section of the literature review.

#### **2.2 Lead Free Solder Alloys**

The main reason for developing lead-free solders is to remove the usage of Lead from the electronic industries and waste disposal process, because of its toxicity. It is impossible to recycle lead Pb which has done in other industries, because the size of the Pb is very small compared to other systems. While electronic material is typically disposed of in landfills, some of it is dumped in densely populated areas, releasing lead Pb vapour into the atmosphere. Additionally, Pb has a substantially greater vapour pressure in the production environment than the majority of other metals. It is also very harmful and hazardous to workers during their inhalation. In contrast, Sn has lower vapor pressure, and is less toxic than Pb element (T. Lee et al., 2010)

In the construction of contemporary electronic circuits, Pb-bearing solders, particularly eutectic or near-eutectic SnPb alloys, have been widely utilized. For the Pb free solders there is a problem which is there are some lacking for Pb-free solders. The qualities of Pb-Sn solder are crucial to a lot of the infrastructure supporting current modern systems. Solders are capable of performing at temperatures that are 80% of their melting point. Two

phases make up the microstructure of sn-pb solder, with the volume ratio of the Sn:Pb-rich phases being roughly 2:1. The majority of the cyclic deformation, which softens the alloy, is carried by the highly soft Pb-rich phase. Because all the plastic deformation occurs in the Sn phase, Sn-based solders have totally different metallurgical properties than Sn-Pb alloys. They small, hard, intermetallic reinforcing particles. Sn-based solders are stronger than Sn-Pb solders because Sn is harder than Pb, which puts additional stress on the surrounding components. This is a difficulty since the design of current die and circuit boards is predicated on the softer characteristics and lower melting point of Sn-Pb. (Lee et al., 2010).

It is necessary to develop effective alternative ways for Pb-free solders for electronic assemblies. There are some needs and requirements for lead free solders. The melting point must be lower so that the heat damage to the assembly being soldered can be prevent. While at the solder joint, the melting point should be high so that it can withstand the operating temperatures. After the solder adequately wets the base metal does a link between the two materials develop. This is ensured by a high Sn concentration, creating a solid connection. The candidate metals should be in sufficient supply or reserve. There is a more supply of antimony (Sb), copper (Cu), zinc (Sn), and zinc (Zn), but a low supply of indium (indium) (In).

Finally, the requirements for manufacturing are discussed to show how implementation of lead-free solders is accomplished. They identified the challenges presented by lead-free solder alloys that possess relatively high temperature and the consequences of using lead-free alloys designed for Sn-Pb soldering to manufacture processes and components. These considerations have led to the introduction of Sn-Cu, Sn-Ag, and Sn-Ag-Cu solders as advancements over Sn- Pb solders. But, as the Sn-content increases, the possibility of void creation, large undercooling at the time of solidification increases (T. Lee et al., 2010).

Table 2.1 Hardness and tensile properties of lead-free solders (Smith & Madeni, 2002)

Chemical Composition	Elastic Modulus		Yield Strength (0.2 % offset)		Tensile Strength		Relative Elongation (%)		Strength Coefficient		Hardening Exponent	
	% by Mass	(ksi)	GPa	(psi)	Mpa	(psi)	Mpa	Uni-form	Total	(psi)		Mpa
Sn-37Pb		2,273	15.7	3,950	27.2	4,442	30.6	3	48	4,917	33.9	0.033
Sn-2Ag-36Pb		2,617	18.0	6,287	43.3	6,904	47.6	1	31	7,223	49.8	0.011
Sn-97Pb		2,753	19.0	1,126	7.8	2,383	16.4	27	38	3,934	27.1	0.235
Sn-3.5Ag.		3,793	26.2	3,256	22.5	3,873	26.7	3	24	4,226	29.1	0.026
Sn-5Sb		6,460	44.5	3,720	25.7	5,110	35.2	3	22	4,177	28.8	0.031
Sn-58Bi.		1,720	11.9	7,119	49.1	8,766	60.4	3	46	9,829	67.8	0.029
Sn-3.5Ag-0.5Sb-1Cd				7,545	52.0				15			
Sn-75Pb				3,426	23.6				53			
Sn-50Bi.				8,263	57.0	8,965	61.8		53			
Sn-52Bi.				6,414	44.2	8,834	60.9		57			
Sn-2Ag-46Bi-4Cu				9,806	67.6	10,070	69.4		3			
Sn-56Bi-2In				7,224	49.8	8,429	58.1		116			
Sn-2Ag-1.5Sb-29Pb				6,489	44.7	6,865	47.3		25			
Sn-3Ag-4Cu.				6,276	43.3	7,006	48.3		22			
Sn-2.5Ag-2Bi-1.5Sb				7,070	48.7	8,117	56.0		21			
Sn-3Ag-1Bi-1Cu-1.5Sb				8,361	57.6	9,256	63.8		21			
Sn-2Ag-9.8Bi-9.8In				14,560	100.4	15,380	106.0		7			
Sn-57Bi-2In				7,304	50.4	8,436	58.2		72			
Sn-2Ag-57Bi				9,487	65.4	10,390	71.6		31			
Sn-57Bi-2Sb				8,521	58.8	9,586	66.1		47			
Sn-57Bi-1Sb				8,285	57.1	8,944	61.7		60			
Sn-2Ag-56Bi-1.5Sb				9,063	62.5	9,946	68.6		27			
Sn-3Ag-55.5Bi-1.5Sb				8,665	59.7	9,379	64.7		45			
Sn-3Ag-55Bi-2Sb				8,984	61.9	9,807	67.6		44			
Sn-3Ag-54Bi-2In-2Sb				5,055	34.9	11,640	80.3		13			
Sn-3Ag-54Bi-2Cu-2Sb				11,440	78.9	12,280	84.7		4			

Table 2.2 The effect of alloy elements on the corrosion of Sn-based lead-free solder alloys (Li et al., 2020)

Solder Alloy	Addition Elements	Microstructure	Resistance to Corrosion	Corrosive Medium
Sn-9Zn	Ti	Refine Zn-rich precipitates; Sn <sub>3</sub> Ti <sub>2</sub> and	Improvement	0.5M Sodium Chloride (NaCl)
Sn-9Zn	Mn	Refine Zn-rich precipitates; Zn <sub>6</sub> Sn <sub>2</sub> Mn	Improvement	0.5M Sodium Chloride (NaCl)
Sn-9Zn	Ga	Refine Zn-rich precipitates	Improvement	3.5wt% Sodium Chloride (NaCl)
Sn-Zn	Zn	Coarse. Zn-rich precipitates	Reduction	0.5M Sodium Chloride (NaCl)
Sn-9Zn	Ni	Refine Zn-rich precipitates; Ni <sub>5</sub> Zn <sub>21</sub>	Improvement	0.5M Sodium Chloride (NaCl)
Sn-9Zn	Cr	Refine. Zn-rich precipitates; Sn <sub>2</sub> Zn <sub>6</sub> Cr	Improvement	0.5M Sodium Chloride (NaCl)
Sn-9Zn	Cu	Refine. Zn-rich precipitates; Cu <sub>5</sub> Zn <sub>8</sub>	Improvement	0.5M Sodium Chloride (NaCl)
Sn-9Zn	Ag	Refine Zn-rich precipitates; AgZn <sub>3</sub>	Improvement	0.5M Sodium Chloride (NaCl)
Sn-Zn	Al	Coarse Zn-rich Precipitates	Reduction	3.5wt% Sodium Chloride (NaCl)
Sn-9Zn	In	Refine Zn-rich precipitates; In <sub>3</sub> Sn	Improvement	6M Potassium Hydroxide (KOH)
Sn-8.5Zn	Cr	Refine Zn-rich precipitates; Cr <sub>2</sub> Sn <sub>2</sub> (Zn)	Improvement	3.5wt% Sodium Chloride (NaCl)
Sn-9Zn	Ni	Ni <sub>3</sub> Sn <sub>4</sub>	Improvement	5wt% Sodium Chloride (NaCl)
Sn-0.7Cu	Fe and Bi	FeSn <sub>2</sub> and Bi-rich Phase	Reduction	3.5wt% Sodium Chloride (NaCl)
Sn-0.7Cu	S	SnS	Improvement	3.5wt% Sodium Chloride (NaCl)
Sn-0.7Cu-0.075Al	Ce and La	Refine grains; CeO <sub>2</sub> and La <sub>2</sub> O <sub>3</sub>	Improvement	3.5wt% Sodium Chloride (NaCl)
Sn-0.7Cu	Al	-	Improvement	Sodium Hydroxide NaOH
Sn-0.7Cu	Al	-	-	Simulated

				seawater
Sn-0.7Cu	Ga	Ga <sub>2</sub> O <sub>3</sub>	Improvement	Simulated seawater
Sn-1.0Ag	Ce	Refine grains and precipitates	Improvement	100mM Na <sub>2</sub> SO <sub>4</sub> + 3mM chloride Ion addition
Sn-3.5Ag	CeO <sub>2</sub>	Refine Ag <sub>3</sub> Sn	Improvement	3.5wt% Sodium Chloride (NaCl)
Sn-Ag	Cu	Coarse Ag <sub>3</sub> Sn and Cu <sub>6</sub> Sn <sub>5</sub>	Improvement	0.1M Sodium Chloride (NaCl)
Sn-xAg	Ag	Volume fraction of the Ag <sub>3</sub> Sn	Improvement	0.3wt% Na <sub>2</sub> SO <sub>4</sub>
Sn-xAg	Ag	Refine Ag <sub>3</sub> Sn and Cu <sub>6</sub> Sn <sub>5</sub>	Improvement	3.5wt% Sodium Chloride (NaCl)
Sn-1.0Ag-0.5Cu	Zn	-	Reduction	3.5wt% Sodium Chloride (NaCl)
Sn-3.0Ag-0.5Cu	Zn and In	-	Reduction	3.5wt% Sodium Chloride (NaCl)
Sn-3Ag-0.5Cu	Al	-	Reduction	3.5wt% Sodium Chloride (NaCl)
Sn-1Ag-0.5Cu	Ni	-	Improvement	3.5wt% Sodium Chloride (NaCl)
Sn-3.0Ag-0.5Cu	Graphene nanosheets	Refine intermetallic compounds	Improvement	3.5wt% Sodium Chloride (NaCl)
95.8Sn-3.5Ag-0.7Cu	NI-coated carbon nanotubes	-	Improvement	3.5wt% Sodium Chloride (NaCl)
Sn-0.3Ag-0.7Cu	Al <sub>2</sub> O <sub>3</sub>	Refine intermetallic compounds	Improvement	0.5M Sodium Chloride (NaCl)
Sn-8.5Zn-xAg-0.1Al-0.5Ga	Ag	-	Improvement	3.5wt% Sodium Chloride (NaCl)
Sn-8.5Zn-0.5Ag-xAl-0.5Ga	Al	-	Improvement	3.5wt% Sodium Chloride (NaCl)
Sn-8.5Zn-0.5Ag-Al-x0.5Ga	Ga	-	Improvement	3.5M Sodium Chloride (NaCl)
Sn-9Zn-3Bi-xCr	Cr	-	Improvement	3.5wt% Sodium Chloride (NaCl)
Sn-9Zn-0.5Ag-1In	In	-	Improvement	3.5wt% Sodium Chloride (NaCl)

### 2.3 Types of SAC Solders (SAC305, SAC387, SAC405, SAC0307)

SAC Alloys are the most popular alloys used to replace tin-lead solders in electronic assembly applications. In applications involving hand soldering, wave soldering, and surface mount technology, these alloys have shown to be effective. SAC Alloys are compatible with current tools, procedures, coatings, and flux chemistries. Bar, cored wire, solid wire, foil, preforms, powder, no clean, water soluble, and RMA solder pastes are all forms in which SAC Alloys are offered. The types of SAC solders were shown in table below.

Table 2.3 Types of SAC Alloys

SAC ALLOYS	TIN	SILVER	COPPER
SAC305	96.50%	3.00%	0.50%
SAC387	95.50%	3.80%	0.70%
SAC405	95.50%	4.00%	0.50%
SAC0307	99.00%	0.30%	0.70%

SAC 305, SAC 0307, and SAC 0307-0.03 P-0.005 Ni electrochemical migration (ECM) behavior has been studied using simulated bodily fluid (SBF) solution. According to the MTTF results, SAC 305's short circuit has the quickest time-to-failure (TTF). When compared to SAC 0307-0.03P-0.005Ni, SAC 305 had a greater corrosion susceptibility. This resulted from the inclusion of nickel and dopant phosphorus in the SAC 0307-0.03 P-0.005 Ni. SAC 305 is an excellent electric conductor, according to the four point-probe test station, but SAC 0307-0.03 P-0.005 Ni is a poor conductor. The alloying element of the solder has an impact on the dendritic development rate. The corrosion resistance of SAC 0307- 0.03P- 0.005Ni in SBF medium is therefore good (Sarveswaran et al., 2017).

Intermetallic (IMC) thickness, morphology, and shear strength of the solder joints of Sn-4.0Ag-0.5Cu/Cu and Sn-4.0Ag-0.5Cu/electroless nickel/immersion silver (ENImAg) were studied. As-reflowed SAC405/Cu and SAC405/ENImAg gave rise to the compounds Cu<sub>6</sub>Sn<sub>5</sub> and (Cu, Ni)<sub>6</sub>Sn<sub>5</sub> IMC, respectively. New layers of Cu<sub>3</sub>Sn and (Ni, Cu)<sub>3</sub>Sn<sub>5</sub> were seen at the interface as the sample grew older. Similar increases in the IMC layer's thickness

and larger grains in proportion to ageing period. Due to the thin layer of IMC and surface quality employed compared to SAC405/Cu, the findings also showed an increase in the shear strength of SAC405/ENImAg. As a result, a ductile fracture at the bulk solder was seen. Overall, the ENImAg surface treatment demonstrated superior solder connection performance than bare Cu (Mohamed Anuar & Osman, 2021).

The impact of thermal ageing on the SAC387 solder alloy's microstructure changes, creep behavior, corrosion characteristics and extensive research was done on the SAC387's creep and corrosion tendencies. The findings show that the fine and planar structures of IMCs are caused by an increase in the thermal ageing temperature of the material. According to the result of the creep test, the alloy samples burst more quickly under the same stress at a higher thermal ageing temperature than they did at a lower thermal ageing ambient temperature. The corrosion experiments also shown that thermal ageing had a substantial impact on the samples' rate of corrosion (Mazullah et al., 2021).

## **2.4 Soldering Technique**

Soldering is a metallurgical joining process that joins two metals by using filler metal. Metal substrates and solder are chemically linked during the formation of intermetallic compounds. Soldering becomes widely used in the electrical industry because it is a process that requires relatively low temperatures for processing because it contains materials with lower melting points (Cong et al., 2019). The solders are heated and completely melted during the soldering process. Molten solders cause the substrates to dissolve in this situation, and as a result, interfacial reactions occur between the solders and the substrates. After cooling, the joints solidify to form solder (L. M. Lee & Mohamad, 2013).

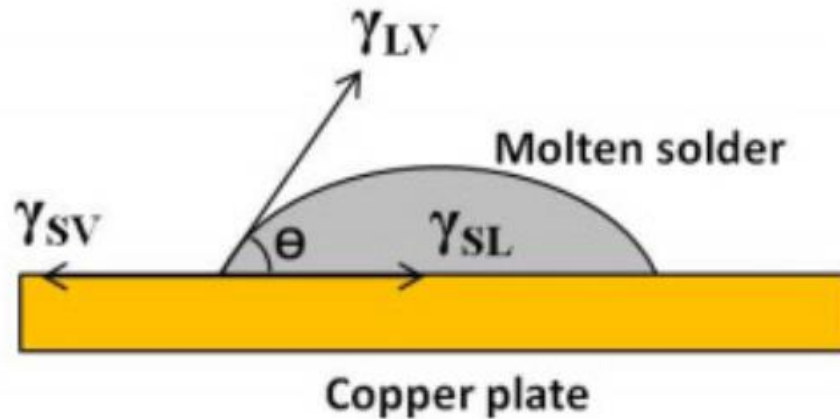


Figure 2. 1: Diagram of Solder on Cu substrate (Comparing Mechanical and Soldering Properties of Alternative Lead-Free Alloys | AIM Solder, n.d.)

Furthermore, soldering does not give any changes in the microstructure of the base metal when it is joined. During solidification, different solid phases are formed, which affects the solder joint properties. Solders, in general, are low melting point alloys because soldering occurs when the solder metal is completely molten. Because most solders are used at relatively high temperatures, they are susceptible to diffusion. In order to achieve effective wetting, interfacial interactions with substrates will be crucial at either the liquid or solid or else the solid or solid contacts at the working temperatures. The design of the land pattern and the metallurgical connection between the component and the board are two elements that have an impact on the solder joint's strength. Reliable solder connections need a strong metallurgical link between the components being connected and the solder.(L. M. Lee & Mohamad, 2013).

### 2.3.1 Reflow Soldering

Reflow soldering is the main method for attaching thousands of small electrical components to printed circuit boards (PCB). The component pads on the PCB are coated with solder paste before (usually via a stencil printing method), and the solder paste

deposits are then covered with the components. The entire assembly is then heated during the reflow process to a temperature that is higher than the melting point (reflow temperature) of the solder alloy.

The most popular method for heating the PCB assembly is to use a furnace with a conveyor belt that travels through many independently programmable heating zones. These heating zones generally use a combination of convective and infrared heat transfer to heat the assembly. Convective heat transmission predominates in more contemporary machines, but older machines often have a substantial component of infrared heat transfer. The product temperature never approaches thermal equilibrium with the heat source, making infrared and convection reflow non-equilibrium thermal processes. Because of this, the temperatures reached in any given assembly rely on both the assembly's heat capacity and the rate of heat transmission into the product.

The recommended technique for soldering surface mount technology components, or SMT, to a printed circuit board, or PCB, is reflow soldering utilizing lengthy industrial convection furnaces. The flow velocity of molten solder onto substrate during reflow soldering gradually decreased due to the rising percentage of nanoparticles in solder alloys. As a result, nanocomposite solder paste's wetting angle increased steadily. The melting behavior was gradually improved by the SAC 305-Fe<sub>2</sub>NiO<sub>4</sub>, SAC 305-NiO, and SAC 305-Fe<sub>2</sub>O<sub>3</sub> composite solder pastes, but not significantly by the SAC 305-ITO composite solder paste. However, the melting temperature of the solder was lowered by the SAC 305-Diamond composite solder paste (Chellvarajoo & Abdullah, 2018).

The eutectic temperature, at which the specific solder alloy transitions from a solid to a liquid or molten state, is what the reflow process aims to achieve with the solder paste. This temperature range causes the molten alloy to exhibit adhesion characteristics. A molten solder alloy has cohesion and adhesion characteristics like those of water. Molten solder alloys will display the phenomenon known as wetting, when within their specified eutectic temperature range, in the condition of liquidus, with enough flux. Due to its thinness, the FPCB demonstrated superior heat absorption and dispersion at lower thicknesses than the thicker one. Importantly, the study advises that the FPCB thickness

should be between 40 and 100 $\mu$ m to maintain the appropriate temperature differential (Ahmad et al., 2021)

The reflow oven temperature's profile is appropriate for a specific circuit board assembly's feature, such as the quantity and size of components, the number of layers present on the board, and the size and depth of the ground plane layer. A certain circuit board's temperature profile will let solder to reflow onto adjacent surfaces without overheating and harming the electrical components beyond their temperature tolerance. Preheat, thermal soak, reflow, and cooling are the four typical zones in the traditional reflow soldering process. Each has a unique thermal profile. (Kementerian Kesehatan Republik Indonesia, 2015)

Five factors were considered for reflowing: peak temperature, soak time, period above liquidus temperature (217°C), cooling rate (gradient of temperature drop off from 225°C to 185°C) and preheat slope (gradient of temperature rise per second from 50°C to 90°C). Figure depicts a typical temperature profile with a peak temperature between 238°C and 247°C, a preheat slope of less than 1.58C/s, and a time above liquid of between 57 and 68 s. (Huang & Lin, 2013).

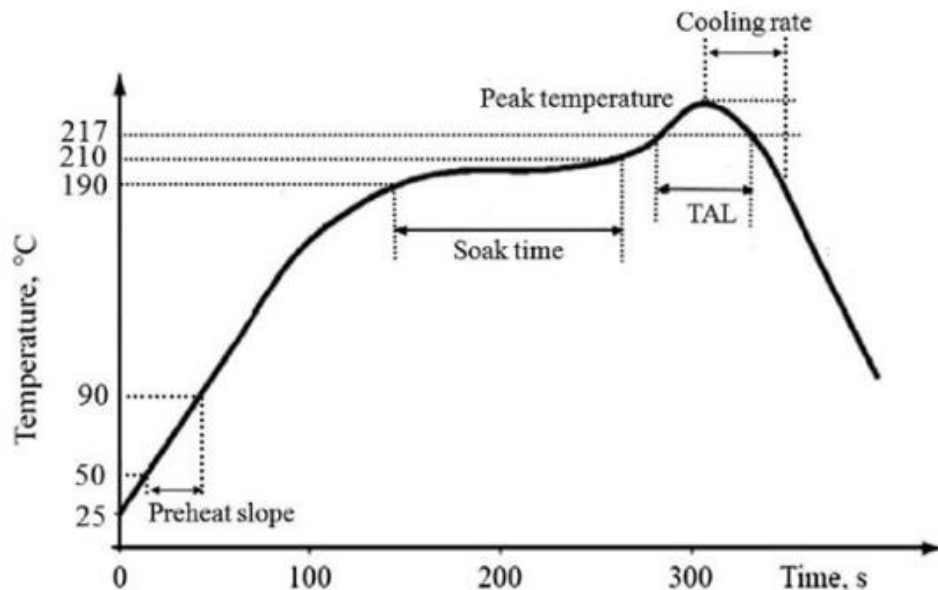


Figure 2. 2: A typical reflow profile (Huang & Lin, 2013)



## 2.4 Intermetallic compound (IMC) layer

IMCs containing Sn are produced in electronic goods using a range of base materials, metallization, and coatings, such as Ag, Cu, Au, Ni, and Ag-Pd. Because solder chemically reacts with conductor metals during soldering, IMCs are likely to grow at the solder or the conductor interface. The presence of intermetallic compounds between conductor metals and solders indicates strong metallurgical bonding. The interfacial IMC layer is a critical factor in solder joint reliability (Jang et al., 2004). As a result, microelectronic assemblies must consider the impact of IMC growth on their reliability and lifetime. An IMC layer must be very thin, continuous, and uniform for better bonding. However, in the absence of IMCs, the solder joint is weak because the plating is not supported by any metallurgical interaction, making electronic packaging dangerous (L. M. Lee & Mohamad, 2013).

Essentially, when Sn-Ag-Cu solder is used to solder a Cu substrate, the Cu begins to dissolve rapidly to the molten solder almost immediately after the flux has removed the oxides and allowed metallurgical contact. There is a rapid rate of dissolution at first. Due to nonequilibrium dissolution, Cu is present in extremely high concentrations at the Cu/liquid interface. Shortly after contact, the molten solder appears supersaturated with dissolved copper (L. M. Lee & Mohamad, 2013).

Solid IMC begins to form in the solder layer adjacent to the contacted metal because of local equilibrium solubility.  $\text{Cu}_6\text{Sn}_5$  crystallites were formed as a result of the chemical reaction between Sn and Cu in the metastable composition. Scallop-type  $\text{Cu}_6\text{Sn}_5$  forms very quickly at the Sn/Cu interface during soldering.  $\text{Cu}_6\text{Sn}_5$  is formed as a result of a chemical reaction following the dissolution of Cu.  $\text{Cu}_3\text{Sn}$ , on the other hand, is formed when  $\text{Cu}_6\text{Sn}_5$  and Cu come into prolonged contact with molten solder.  $\text{Cu}_3\text{Sn}$  is formed as a result of diffusion and reaction type growth (L. M. Lee & Mohamad, 2013).

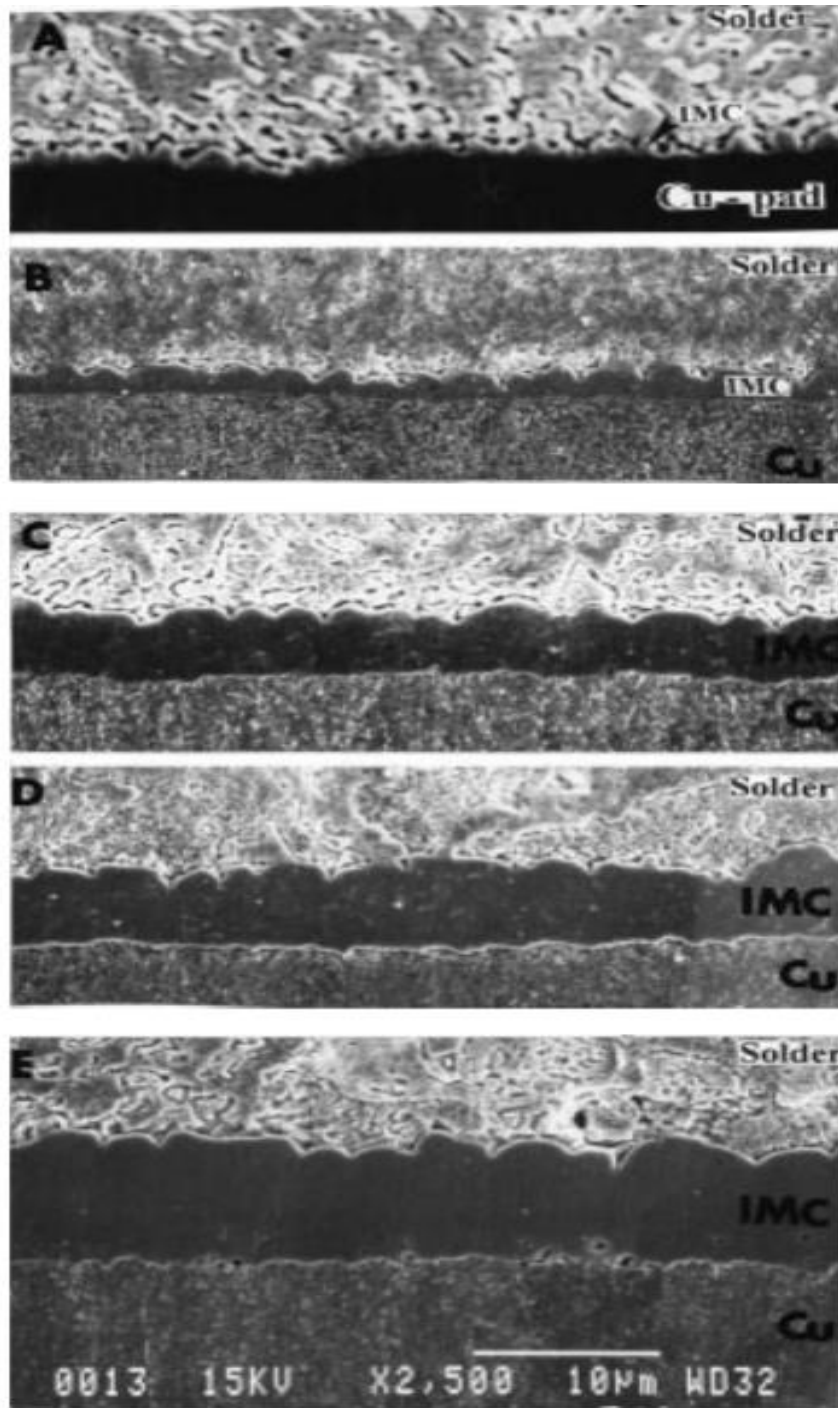


Figure 2. 4: SEM image of Intermetallic Compound (Chan et al., 1997)

Intermetallic compounds (IMCs) are solid-state compounds formed by the reaction of molten solder alloy with metal substrates. IMCs usually form between the solder and the substrate. According to (Chan et al., 1997). The intermetallic reduces solder joint lifetime, with the reduction increasing with IMC thickness and, thus, ageing time. Failure-related cracks begin primarily beneath the component metallization and grow along the IMC/solder interface. Thus, for shear cycling, the morphology of the Cu–Sn intermetallic compounds/bulk solder interface, as well as the IMC layer thickness, affect the lifetime of the solder joint. Fatigue lifespan suffers from an IMC/solder boundary that is flat. The CuSn -phase generated during storage and prolonged operation has only a little impact on lifespan until it completely consumes the tin in the solder beneath the component metallization.

## **2.5 Hardness Test**

Hardness is the characteristics of solid materials that offer resistance when a force is applied. According to materials science, hardness may be classified into three categories: Among these are (I) indentation hardness, which measures resistance to plastic deformation brought on by a constant load; (II) rebound hardness, which measures how high an object bounces after being dropped on the material; and (III) scratch hardness, which measures resistance to fracture or plastic deformation brought on by friction from a sharp object (Riggio & Piazza, n.d.)

On the other hand, as the dependability and structural stability of the component are greatly influenced by the mechanical characteristics, knowledge on the material's mechanical properties is crucial when designing a structural component for electronic devices. According to the process for reinforcing grain boundaries in metallic materials, the mechanical characteristics are directly connected to their average grain size. Most of the time, the average grain size affects the microhardness (Jiang et al., 2020). Examples of applications include small parts, thin, superficially hardened parts, plated surfaces, and individual material components. Rockwell, Brinell, and Vickers tests are a few examples of macro hardness testing. Knoop diamond and the Vickers diamond pyramid are used for microhardness testing.

### 2.5.1 Vickers Hardness Test

Vickers test is the one of the earliest techniques of hardness testing, which uses a wide hardness scale appropriate for most metals. In the Vickers hardness test, a  $136^\circ$  pyramidal diamond indenter that creates a square indent is employed. For 10 to 15 seconds, the load is applied.

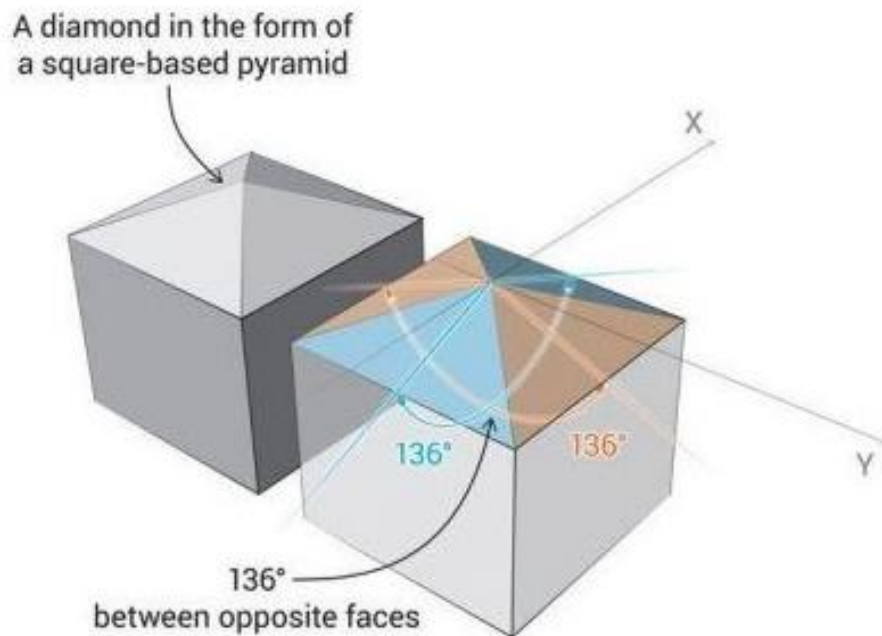
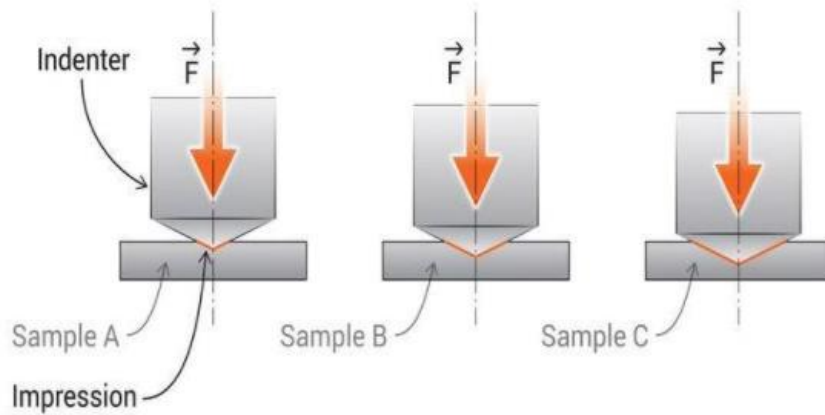


Figure 2. 5: Vickers Hardness Test indenter geometry. Image is © 2017 EngineeringClicks

The two diagonal lengths of the test surface are measured, and the average is used to calculate the hardness, which is represented by the  $F/A$  ratio (where  $F$  is the force or load, in kgf; and  $A$  is the surface area of the indentation, in mm<sup>2</sup>). The dimension ( $d$ ) and a calibration for various kilograms weights are obtained by averaging the two axes of the diamond-shaped indentation, which is measured in millimeters ( $P$ )(Campo, 2008) Hardness (HV) is expressed as a number, such as HV 2 for a 2 kg load or HV 6 for a 6 kg load. Vickers hardness can be calculated using formula which has shown bellow:

$$HV = \frac{2F \sin \frac{136^\circ}{2}}{d^2} = 1.854 \frac{F}{d^2}$$



### Measurement of impression diagonals

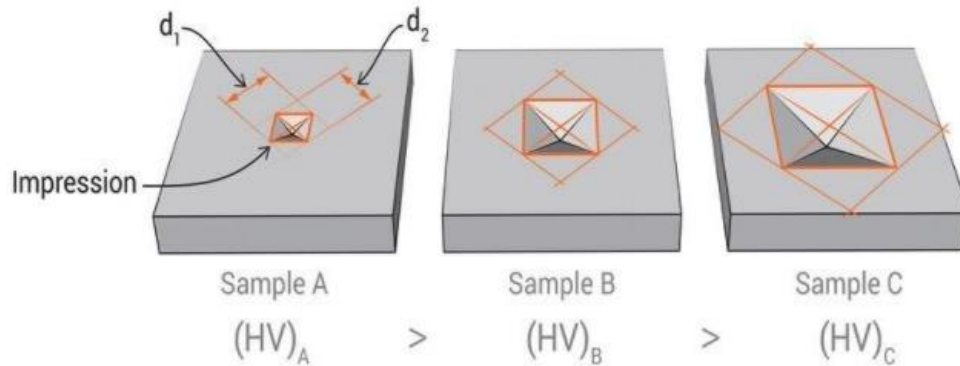


Figure 2. 6: Vickers Hardness Test indentation examples. Image is © 2017 EngineeringClicks

The Vickers micro hardness test is extremely useful, and it has been used in Pb free solder characterizations. Technically, the hardness of the bulk solder alloy and solder joints can be evaluated. For the bulk alloy, the average hardness of the lead-free solder alloy sectioned from the ingot or as-cast is frequently measured using the Vickers hardness scale. In terms of solder joints, the average hardness of the interconnections produced by paste printing and reflowing was determined (Chew et al., 2015) (Yahaya & Mohamad, 2017).

The hardness test was performed by (Singh, 2018) reported that used the Vickers hardness with an average of five 1 kgf load indentation to conduct the hardness test. The SAC solder alloy produces a high hardness average of 14.40Hv, indicating its dependability in terms of resistance to deformation. This is primarily due to the microstructure and SEM image showing a well-defined and wider eutectic phase containing intermetallic compounds of  $\text{Cu}_6\text{Sn}_5$  and  $\text{Ag}_3\text{Sn}$ .

### **2.5.2 Microhardness**

Microhardness is the hardness of a material as measured by instruments equipped with small indenters. As a result, less force is applied in comparison to standard measuring instruments, allowing measurements on thinner sheets or smaller test materials that may not respond accurately to standard measurements. The indentations are typically so minute that precise measurements need to be taken using a microscope. Resistance to densification, cracking, and deformation is indicated by the microhardness rating. It is regularly employed to assess the mechanical qualities of metal materials. (Tang et al., 2014). When testing materials such as metals, the microhardness has a linear correlation with the tensile strength.

Figure 2.7 illustrates how the solder matrix's microhardness increased as a result of the inclusion of  $\text{TiO}_2$  nanoparticles. The maximum microhardness value is 17.6 0.63 Hv for SAC-0.5 $\text{TiO}_2$ . In comparison to the SA and SAC solders, the microhardness of the  $\text{Sn}_{3.5}\text{AgXCu}$  composite solders rose by 15.5 percent ( $X = 0$ ) and 16.6 percent ( $X = 0.7$ ), respectively. depending on (Chang et al., 2011).

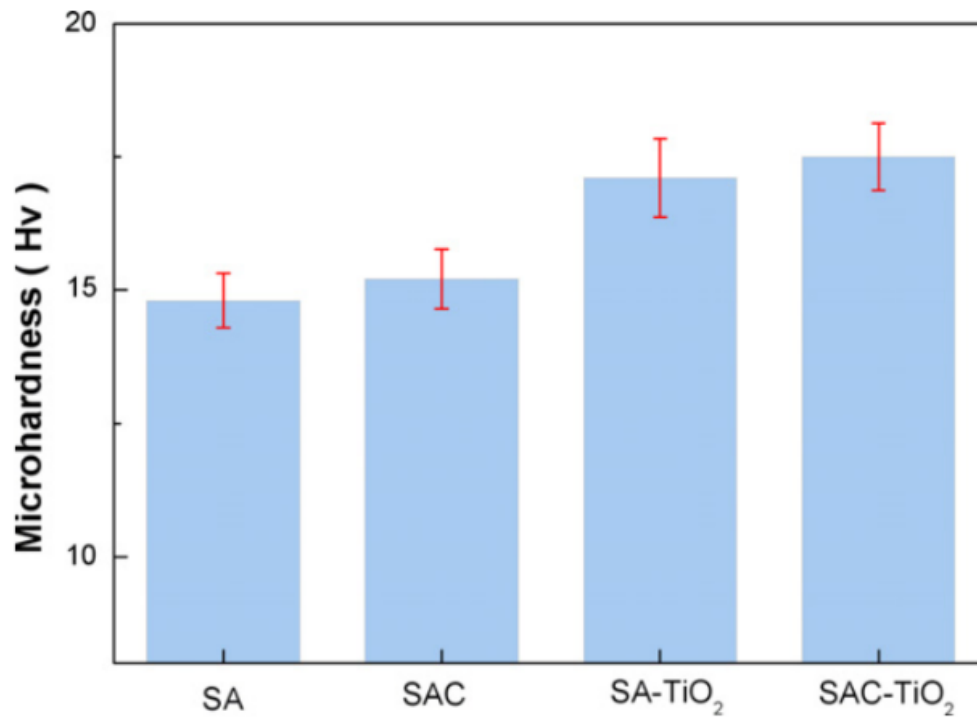


Figure 2. 7: Bar graph showing the impact of TiO<sub>2</sub> nanoparticles on its microhardness of the Sn<sub>3.5</sub>AgxCu solders (Chang et al., 2011).

Figure 2.8 illustrate how TiO<sub>2</sub> nanoparticles affect the microhardness of Sn-3.0Ag-0.5Cu-xTiO<sub>2</sub> composite solders. The microhardness of the composite solder ranges from 14.10Hv to 19.30Hv and rises with increasing weight percentages of TiO<sub>2</sub> nanoparticles, reaching a peak at 0.1 wt. percent. Even while the microhardness somewhat declines when the TiO<sub>2</sub> nanoparticle concentration is raised, it still outperforms that of TiO<sub>2</sub>-free solder. The microhardness improvement of these TiO<sub>2</sub>-containing composite solders is also shown to be 19-37 percent higher than that of TiO<sub>2</sub>-free non-composite solder, according to (Tang et al., 2014).

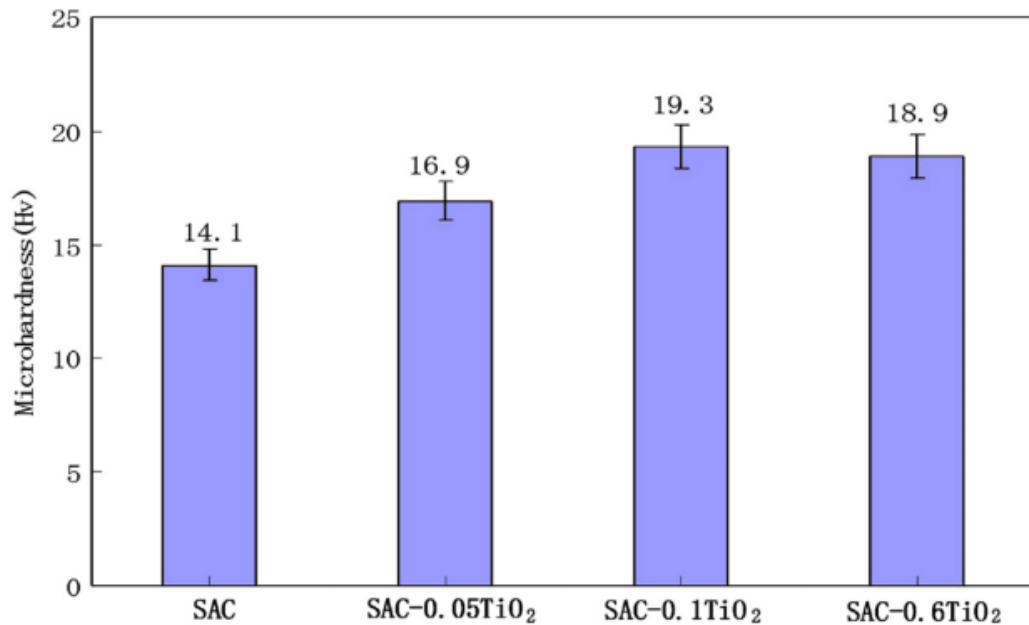


Figure 2. 8: The graph showing the effect on the addition of TiO<sub>2</sub> nanoparticle on the microhardness of the Sn-3.0Ag-0.5Cu-xTiO<sub>2</sub> composite solders (Tang et al., 2014).

By comparing (Chang et al., 2011), (Chang, Jain et al. 2011) microhardness, SAC solder has higher microhardness than SA solder. The addition of 0.5wt% TiO<sub>2</sub> nanoparticles improves the microhardness of both SA and SAC composite solder from  $14.8 \pm 0.51$  Hv and  $15.1 \pm 0.74$  Hv to  $17.1 \pm 0.56$  Hv and  $17.6 \pm 0.63$  Hv respectively. From the result (Tang et al., 2014), microhardness increases with increasing TiO<sub>2</sub> nanoparticle weight percentage in Sn-3.0Ag-0.5Cu-xTiO<sub>2</sub> composite solder, reaches maximum value of 19.30Hv at 0.1wt.% TiO<sub>2</sub> nanoparticles addition. When compared to TiO<sub>2</sub>-free solder, the microhardness of TiO<sub>2</sub>-containing composite solders is increased by 19–37%. This obvious strengthening effect could be attributed to a decrease in the spacing between the Ag<sub>3</sub>Sn grains.

### 2.5.3 Nanohardness

Nanohardness testing refers to hardness tests in which the indentation depth is typically less than about 50nm, or the indentation diameter or length is less than about 150nm (Sundararajan & Roy, 2001). Nanohardness is a popular technique for determining the local stress, strain, modulus, and toughness of materials.

While studying effect of microwave hybrid heating on the formation of intermetallic compound of Sn-3.0Ag-0.5Cu/Cu joint, (Lutfi et al., 2015) conducted the nanohardness of the joints of Sn-Ag-Cu Solder using a nanohardness tester. The average nanohardness value of Cu<sub>6</sub>Sn<sub>5</sub> IMC rose when 4g of graphite powder was present; it went from 19.42 GPa to 20.69GPa to 22.09GPa with increasing microwave heating durations. Cu<sub>6</sub>Sn<sub>5</sub> IMC's hardness value in 6g of graphite powder grew from 11.16 GPa to 14.75 GPa to 17.44 GPa as the heating time and cooling time increased. The data in this section demonstrates that the Cu<sub>6</sub>Sn<sub>5</sub> IMC hardness values were greater when heated with 4g of graphite powder than when heated with 6g of graphite powder (figure 2.9a). The results show that heating Cu<sub>6</sub>Sn<sub>5</sub> IMC with 4g of graphite powder is more stable due to the uniformity of Cu<sub>6</sub>Sn<sub>5</sub> IMC scallop-like structure at the Sn-3.0Ag-0.5Cu joint interface (Lutfi, Yusof et al. 2014).

The nano hardness and elastic modulus of Bi and Ni doped SAC solders are found to be greater than those of the original solders. The SAC, SAC-Ni and SAC-Bi composite solders have the hardness of  $0.16 \pm 0.005$  (GPa),  $0.18 \pm 0.02$  (GPa),  $0.36 \pm 0.022$  (GPa) as shown in (figure 2.9b). As a result, minor alloying additions of Ni or Bi can significantly improve the nanomechanical properties of SAC solders. SAC-Bi solders have a higher nano hardness value than others by about 0.4 GPa. The solid strengthening effect of Bi is generally attributed to the significant improvement in nano hardness of SAC solders (Lin et al., 2018).

The average hardness value in all horizontal cross-sections of the composite SAC305-1.0TiO<sub>2</sub> solder alloy was found to be greater than that of the SAC305 alloy. Nanoindentation was conducted to compare and study the effect on hardness properties with the presence of TiO<sub>2</sub> nanoparticles in SAC composite solder in four different cross-section area. The hardness value of SAC305 and SAC305-1.0TiO<sub>2</sub> solder alloy at